Surface & Coatings Technology 342 (2018) 167–177

Contents lists available at ScienceDirect

Surface & Coatings Technology

journal homepage: www.elsevier.com/locate/surfcoat

Tribological mechanism of diamond-like carbon films induced by Ti/Al co-doping

Cuicui Kong[a,b], Peng Guo[a], Lili Sun[a], Yong Zhou[a,d], Yunxiao Liang[b], Xiaowei Li[a,c,*], Peiling Ke[a], Kwang-Ryeol Lee[c], Aiying Wang[a,**]

[a] Key Laboratory of Marine Materials and Related Technologies, Zhejiang Key Laboratory of Marine Materials and Protective Technologies, Ningbo Institute of Materials Technology and Engineering, Chinese Academy of Sciences, Ningbo 315201, China
[b] Faculty of Materials Science and Chemical Engineering, Ningbo University, Ningbo 315201, China
[c] Computational Science Center, Korea Institute of Science and Technology, Seoul 136-791, Republic of Korea
[d] School of Materials Science and Engineering, Shanghai University, Shanghai 200444, China

ARTICLE INFO

Keywords:
Diamond-like carbon
Ti/Al co-doped
Tribological behaviors
Transfer layer

ABSTRACT

Co-doping two metals into diamond-like carbon (DLC) films exhibits a desirable combination of low residual stress and hard hardness for further application, but the insight into tribological mechanism induced by the co-doped metals is still not fully clarified yet. In this work, we fabricated the Ti/Al co-doped DLC films (Ti/Al-DLC) with various metal concentrations using the hybrid ion beam system, and the tribological properties of films were systematically investigated. Results revealed that the co-doped Ti/Al metals played an important role in the tribological behaviors of DLC films; the film deposited at 2.5 A ($Ti_{10.06at.\%}Al_{4.78at.\%}$) exhibited the lowest friction coefficient of about 0.05 and wear rate of $1.56 \times 10^{-16}\ m^3\ N^{-1}\ m^{-1}$. This attributed to the formation of thick transfer layer in the friction interface, which could be described as a dual or hierarchy nanostructure constructed of cross-linking amorphous carbon networks and hard phase (mainly TiC and Al_2O_3) structures.

1. Introduction

Diamond-like carbon (DLC) films have received widespread attention due to its excellent properties, including high hardness, chemical inertness, wear resistance and low friction [1,2]. As for the practical application, metal-doped DLC (Me-DLC) films have been more widely used, since the incorporation of metal elements can effectively overcome the intrinsic defects of DLC film such as high residual stress and improve its mechanical and tribological performance. Generally, according to the bond characteristics between the metal and C atoms, the doped metals can be mainly divided into two groups. One is the strong-carbide-forming (SCF) metal such as Ti [3], W [4], Cr [5], etc., which tends to form the carbide nanocrystallite in amorphous carbon matrix following the superior hardness, toughness and wear resistance, but the strong Me—C bonding also leads to the increased residual compressive stress. The other group is called as the weak-carbide-forming (WCF) metal including Al [6], Cu [7], Ni [8] and so on, which exists in the form of weak anti-bonding or ionic bond with C atom, resulting in the significant reduction of residual compressive stress and the improvement of toughness and tribological properties, but it also deteriorates the hardness seriously. Therefore, mono-doping SCF or WCF metal into amorphous carbon structure seems to be an ineffective way to obtain the excellent comprehensive properties of DLC films for the complicated applications such as cutting tools and automobile components [9].

Recently, co-doping SCF/WCF metals into DLC has been attempted to meet the requirement for both the outstanding mechanical and tribological properties. For example, Zhou et al. [10] reported that the DLC film co-doped by W/Al exhibited superior mechanical properties, lower friction coefficient (~0.05) and specific wear rate ($\sim 1.8 \times 10^{-16}\ m^3\ N^{-1} m$) compared to the pure and Al or W mono-doped DLC films, and the excellent tribological properties attributed to the graphitic transfer layer formed on the friction contact surfaces. Paranjayee Mandal and co-workers [11] studied the tribological behavior of Mo/W co-doped DLC film under ambient condition, and found that the transfer layer consisted of two types of oxides, among which the MoO_3 and Magnéli phase oxides acted as solid lubricants due to their layered structure. Liu and co-workers [12] showed that Si/Al co-doping could enhance the elastic recovery rate of DLC film to be beyond 84%, and the super-low friction (< 0.01) and wear resistance were also

* Correspondence to: X. Li, Computational Science Center, Korea Institute of Science and Technology, Seoul 136-791, Republic of Korea.
** Corresponding author.
E-mail addresses: lixw0826@gmail.com (X. Li), aywang@nimte.ac.cn (A. Wang).

https://doi.org/10.1016/j.surfcoat.2018.02.098
Received 17 January 2018; Received in revised form 25 February 2018; Accepted 27 February 2018
Available online 28 February 2018

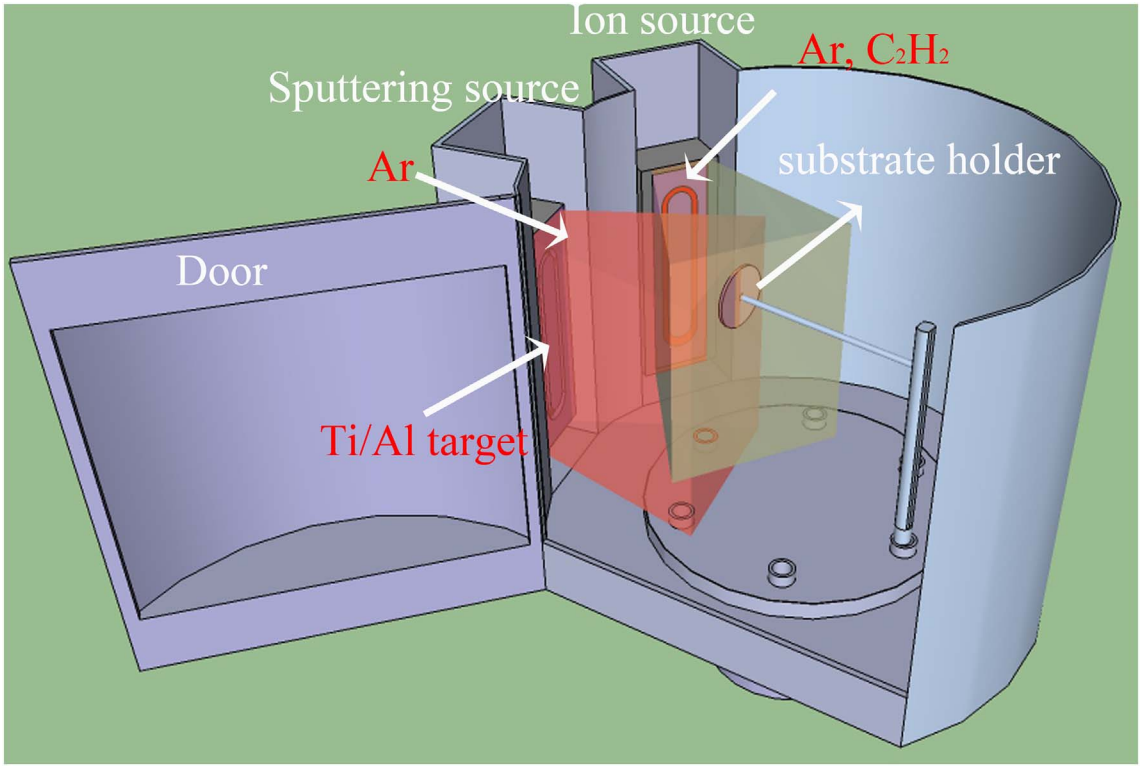

Fig. 1. Schematic diagram of the hybrid deposition system.

Table 1
Process parameters for Ti/Al interlayer.

	Sputtering current/A	Ar flow/ sccm	Working pressure/Pa	Bias voltage/V	Deposition time/min
Parameters	4	55	0.43	−100	16

obtained, which was attributed to the enhancement of Al incorporation on the graphitization of contact layer during tribo-tests. Li et al. [13] carried out ab-initio calculations and confirmed that Ti/Al co-doping could result in the significant residual stress reduction without deteriorating the mechanical properties, and the stress reduction was attributed to the critical relaxation of distorted C—C bond lengths as well as the formation of weak Me—C bond characteristics. Chi-Lung Chang et al. [14] also reported that Ti/Al-doped DLC films exhibited the lower friction coefficient at approximately 0.15 due to the presence of graphite. Hence, the SCF/WCF metal co-doping could enhance the comprehensive properties of DLC films, but the tribological mechanism of films caused by co-doped metals is not fully clarified yet due to the strong dependence on the kinds and concentrations of doped metals; in particular, the effect of each doped metal on the friction process is still unclear.

In our previous studies [15,16], we have successfully fabricated Ti/Al-DLC films with different Ti/Al concentrations by hybrid ion beam deposition system, and also systematically investigated the dependence of mechanical properties on different process parameters. So, in the present work, we prepared the Ti/Al-DLC films by hybrid ion beam deposition system, and focused on the exploration of Ti/Al induced tribological mechanism of DLC films by the in-depth analysis of worn interfaces and products. It was observed that the tribological properties were strongly sensitive to the chemical state of co-doped Ti/Al atoms and corresponded structural evolution.

2. Experimental methods

2.1. Preparation of Ti/Al-DLC films

DLC films with different Ti/Al concentrations were deposited on silicon P (100) wafers using hybrid ion beam deposition system compositing of linear anode-layer ion source (ALIS) supplied with C_2H_2 gas for DLC film deposition and DC magnetron sputtering unit provided with a Ti/Al composite target (50/50 at.%), as shown in Fig. 1. After ultrasonic cleaning in acetone for 15 min and drying in air, the Si wafers were put into the vacuum chamber, the distances from substrate to ALIS and Ti/Al target were kept at about 20 cm separately (Fig. 1). Prior to deposition, the chamber was evacuated to about 2.7×10^{-3} Pa. Then the substrates were etched using Ar^+ bombardment for 15 min at bias voltage of −100 V to remove the surface impurities. After that, a Ti/Al interlayer with thickness of about 450 ± 20 nm was deposited on the substrates using magnetron sputtering at the bias voltage of −100 V, Ar gas flow of 55 sccm and sputtering current of 4.0 A, respectively (Table 1). During the film deposition process, 70 sccm Ar and 10 sccm C_2H_2 gas were introduced into the magnetron sputtering source and ALIS separately, and the detailed process parameters can be found in Table 2. Particularly, the deposition time under different sputtering currents was controlled for the same thickness in order to avoid the effect of film thickness on the structural properties.

Table 2
Deposition parameters for Ti/Al-DLC films.

	Sputtering current/A	LIS working current/A	Bias voltage/V	LIS working voltage/V	Working pressure/Pa	Deposition time/min
Parameters	1.0, 2.0, 2.5, 3.0	0.2	−50	1400 ± 50	0.56	104, 76, 67, 45

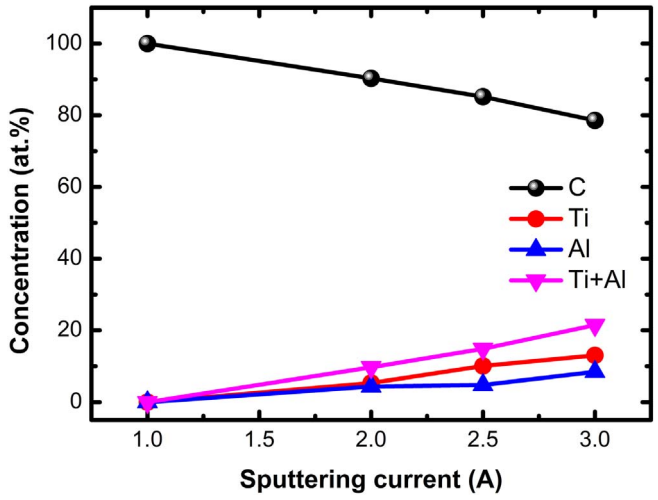

Fig. 2. Compositions of the films as a function of sputtering currents.

2.2. Tribological property tests

The tribological behaviors of Ti/Al-DLC films were evaluated on a ball-on-disk reciprocating tribometer (Center for Tribological UMT-3) at room temperature, with relative humidity of about 86% under dry sliding conditions. A steel ball (GCr15, HRC60) with diameter 6 mm was used as the counter body. All tests were performed at sliding velocity of 5 cm/s for a sliding time of 1800 s and the applied load was 20 N; the length of wear track was 5 mm and the reciprocating frequency was 5 Hz. After tests, the surface profiles of wear tracks were measured by surface profilometer (Alpha-Step IQ). The wear rates of tested films were calculated using the following equation

$$K = \frac{V}{L \times N} \quad (1)$$

where K is wear rate, V is wear volume loss, N is normal load, L is total sliding distance. V could be calculated by plotting length and cross-sectional worn area of the wear track.

2.3. Composition and microstructure characterizations

The thickness of deposited films was measured by surface profilometer with employing a step formed by a showdown mask. X-ray photoelectron spectroscopy (XPS, Thermo Scientific ESCALAB 250) with Al (mono) Kα irradiation at pass energy of 160 eV was used to analyze the composition and chemical bonds of the deposited films and worn products. Before commencing the measurement, the film surface was etched by Ar^+ ion beam to remove the contaminants. Raman spectroscopy (Renishaw, inVia-reflex) at 532 nm wavelength was used to assess the carbon atomic bonds of original Ti/Al-DLC and transfer layers. Combined with the X-ray energy dispersive spectroscopy (EDS), scanning electron microscopy (SEM) was utilized to analyze the wear scar on steel balls after tribological test. Furthermore, the microstructural characterization was performed by high-resolution transmission electron microscopy (HRTEM, FEI Tecnai F20), and the specimens from wear scar and wear track were prepared by Focused Ion Beam (FIB) instrument (Carl Zeiss, Auriga) and a protective layer of Pt mixed was firstly deposited onto the sample surface before FIB experiment.

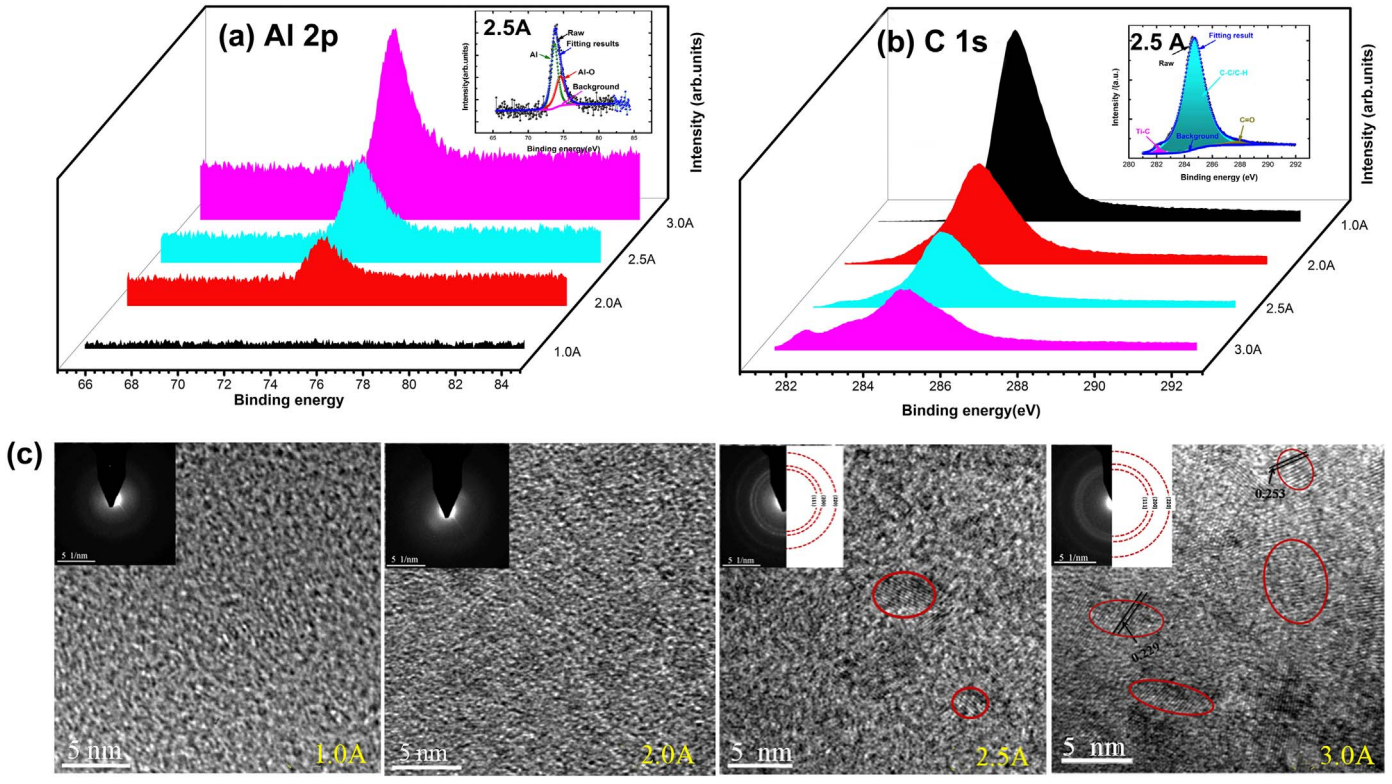

Fig. 3. (a) Al2p spectra of Ti/Al-DLC films and in which the inset was the deconvolution of Al2p XPS spectra for the film deposited at 2.5 A; (b) C1s spectra, in which the inset was the deconvolution of C1s spectra for film deposited at 2.5 A; (c) the HRTEM images and corresponding SAED pattern of films deposited at sputtering current of 1.0, 2.0, 2.5 and 3.0 A, respectively.

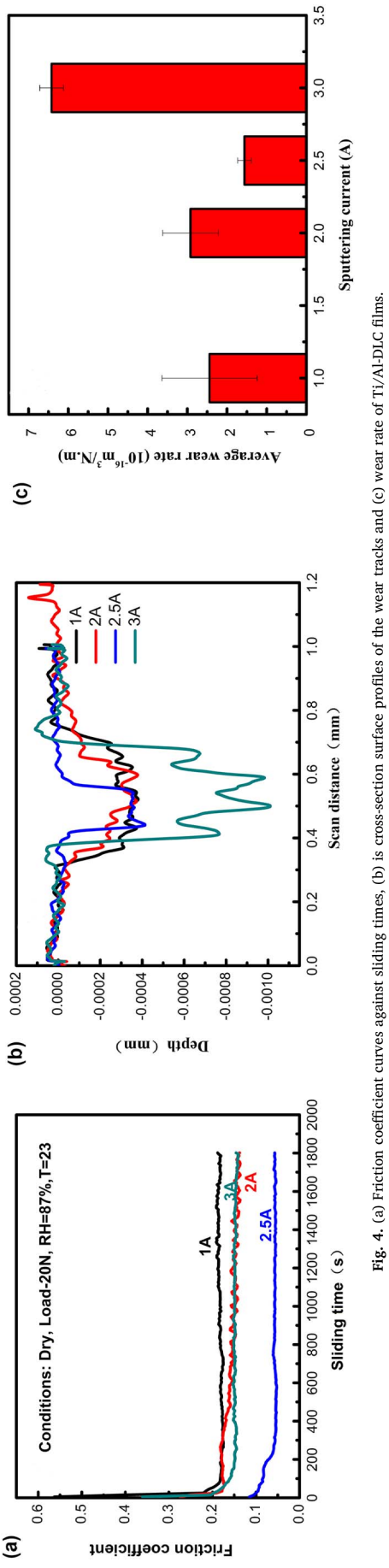

Fig. 4. (a) Friction coefficient curves against sliding times, (b) is cross-section surface profiles of the wear tracks and (c) wear rate of Ti/Al-DLC films.

3. Results and discussion

3.1. Thickness and composition

As the sputtering current was changed from 1.0 to 3.0 A, the film thickness was kept around 1600 nm by changing the deposition time, which minimized the thickness dependence of structure and properties. Fig. 2 shows the Ti, Al and C concentrations in Ti/Al-DLC films as a function of the sputtering current. With increasing the sputtering current, Ti and Al concentrations increased monotonously, which was attributed to the enhanced bombardment effect of Ar ions on the Ti/Al composite target; when the sputtering current is 2.5 A, the doped Ti and Al concentrations were 10.06 at.% and 4.78 at.%, respectively.

3.2. Microstructure

Fig. 3 shows the XPS spectra of Ti/Al-DLC films including Al 2p and C 1s, respectively. In Al 2p spectra (Fig. 3a), there was a peak with binding energy ranging from 72 to 77 eV when the sputtering current is higher than 1.0 A, which could be deconvoluted into two peaks at around 73.6 eV for pure Al and 74.3 eV for Al—O bond separately (inset of Fig. 3a) [14,17]. This indicated that the doped Al atoms existed in the state of pure and oxidized Al clusters without carbide formed. In Fig. 3b, the C 1s spectra revealed a major peak located at the binding energy of 284.5 eV, which was assigned to C—C/C—H [12,18]. With increasing the sputtering current from 1.0 to 3.0 A, the intensity of C1s peak decreased due to the reduction of C concentration in the films; when the sputtering current was 2.5 A, a shoulder peak at around 282.2 eV appeared (inset of Fig. 3b), which corresponded to the Ti—C bond [19–21], and this peak intensity became more prominent with further increasing the sputtering current to 3.0 A. This result demonstrated that when the sputtering current was lower than 2.5 A, Ti atoms were only dissolved in the amorphous carbon and there was no crystalline structure distinguished from the HRTEM images (Fig. 3c). However, as the sputtering current increased to be larger than 2.5 A, Ti atoms began to bond with carbon atoms and existed in the form of titanium carbide in the amorphous carbon matrix, and the further analysis of HRTEM images and corresponding selective area electron diffraction (SAED) in Fig. 3c also confirmed the appearance of titanium carbide polycrystalline phases, in which the sharp crystalline diffraction rings were identified to be (111), (200), (220) and (222) reflections of cubic TiC crystallites, respectively [15].

3.3. Tribological properties

The tribological properties of Ti/Al-DLC films are presented in Fig. 4. As shown in Fig. 4a, as the sputtering current increased from 1.0 to 2.5 A, the friction coefficient dropped from 0.18 to 0.05, and then increased to 0.15 with further increasing the sputtering current to 3.0 A. From the 2D cross-section surface profiles of wear tracks (Fig. 4b), the films deposited at 1.0 and 2.0 A displayed broad and shallow wear tracks with width of around 0.45 mm and depth of 400 nm; while the wear track became much narrower for the film at 2.5 A, which was about 1/3 width of that at 1 A; as the sputtering current was 3.0 A, the deepest wear depth of around 1000 nm was generated. According to the wear tracks, the wear rate for each case was calculated by the Eq. (1), as illustrated in Fig. 4c. It could be observed that the minimal value of $1.56 \times 10^{-16}\ m^3\ N^{-1}\ m^{-1}$ was also obtained at 2.5 A. Hence, the Ti/Al-film deposited at 2.5 A had the best anti-friction and wear resistance performance.

3.4. Tribological mechanism

In order to clarify the tribological mechanism of DLC films induced by Ti/Al co-doping, the structure of wear tracks was analyzed first. The

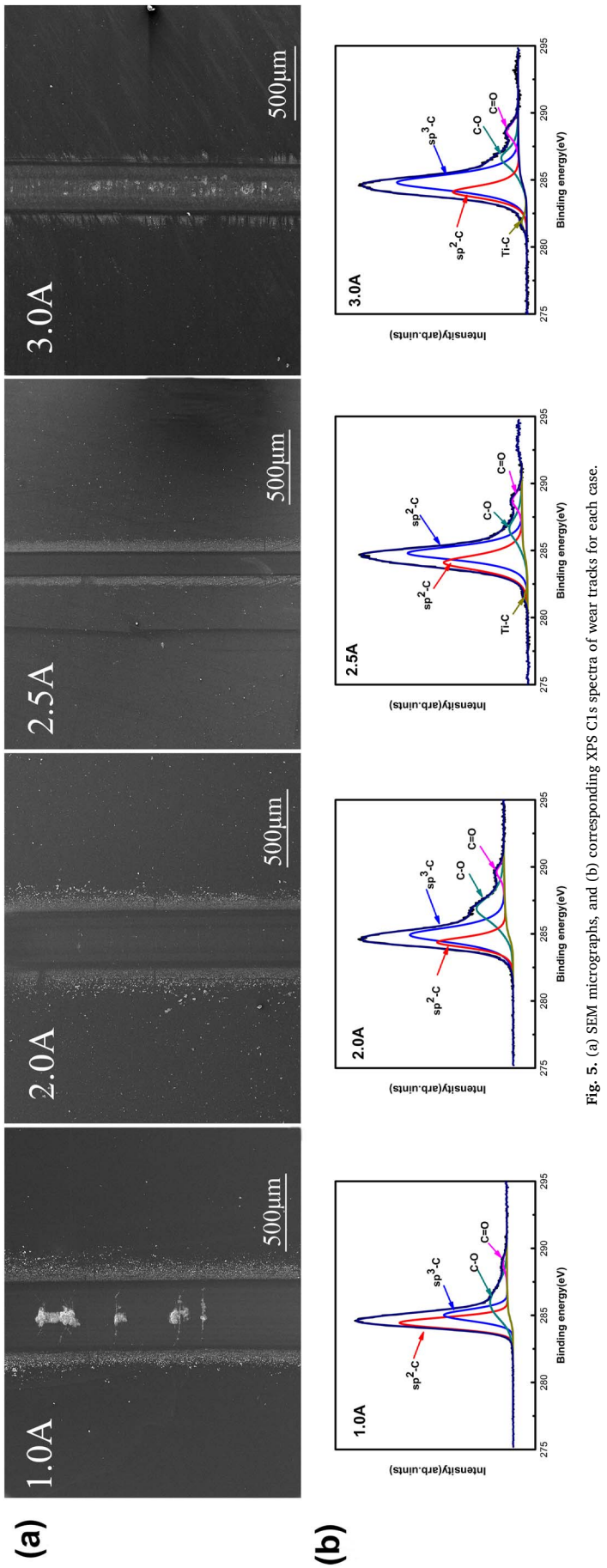

Fig. 5. (a) SEM micrographs, and (b) corresponding XPS C1s spectra of wear tracks for each case.

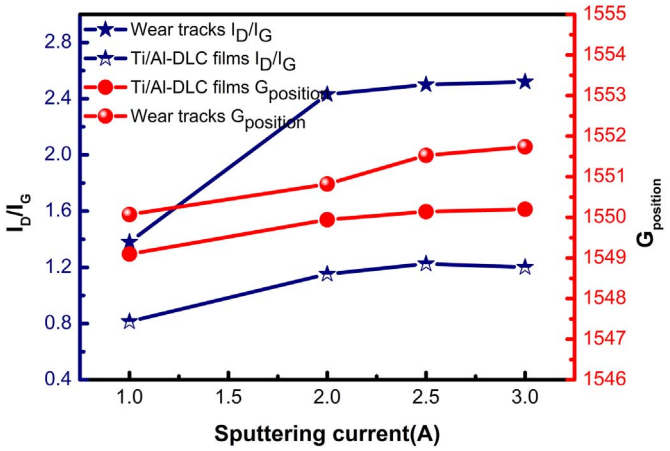

Fig. 6. I_D/I_G of as-deposited Ti/Al-DLC and corresponding wear tracks as a function of sputtering current.

morphologies in Fig. 5a showed that compared with other cases, the film at 2.5 A produced the narrowest wear track, while there was much wear debris accumulated in the middle of wear tracks at 1.0, 2.0 and 3.0 A, respectively. In order to investigate the chemical evolution of wear tracks for each case, the XPS characterizations on the wear tracks are carried out in Fig. 5b. The C 1s spectra from wear tracks showed the same variation trend as the as-deposited cases. Taking the film at 2.5 A for example, the C 1s spectra of wear track was also deconvoluted into four peaks, corresponding to Ti—C, C—C/C—H, C—O and C═O bonds, respectively.

Raman spectroscopy is a powerful tool to obtain the evolution of carbon bonding structure of DLC films. The Raman spectra for the as-deposited films and wear tracks were obtained separately (see Fig. S1 in Supporting Information), and then further fitted into D peak (centered at about 1350 cm^{-1}) and G peak (centered at about 1580 cm^{-1}). The intensity ratio of D peak to G peak, I_D/I_G and G peak position are illustrated in Fig. 6. It is empirically known that the I_D/I_G and G peak position increase as the increase of graphitic component in DLC films. For the as-deposited films, the I_D/I_G ratio with sputtering

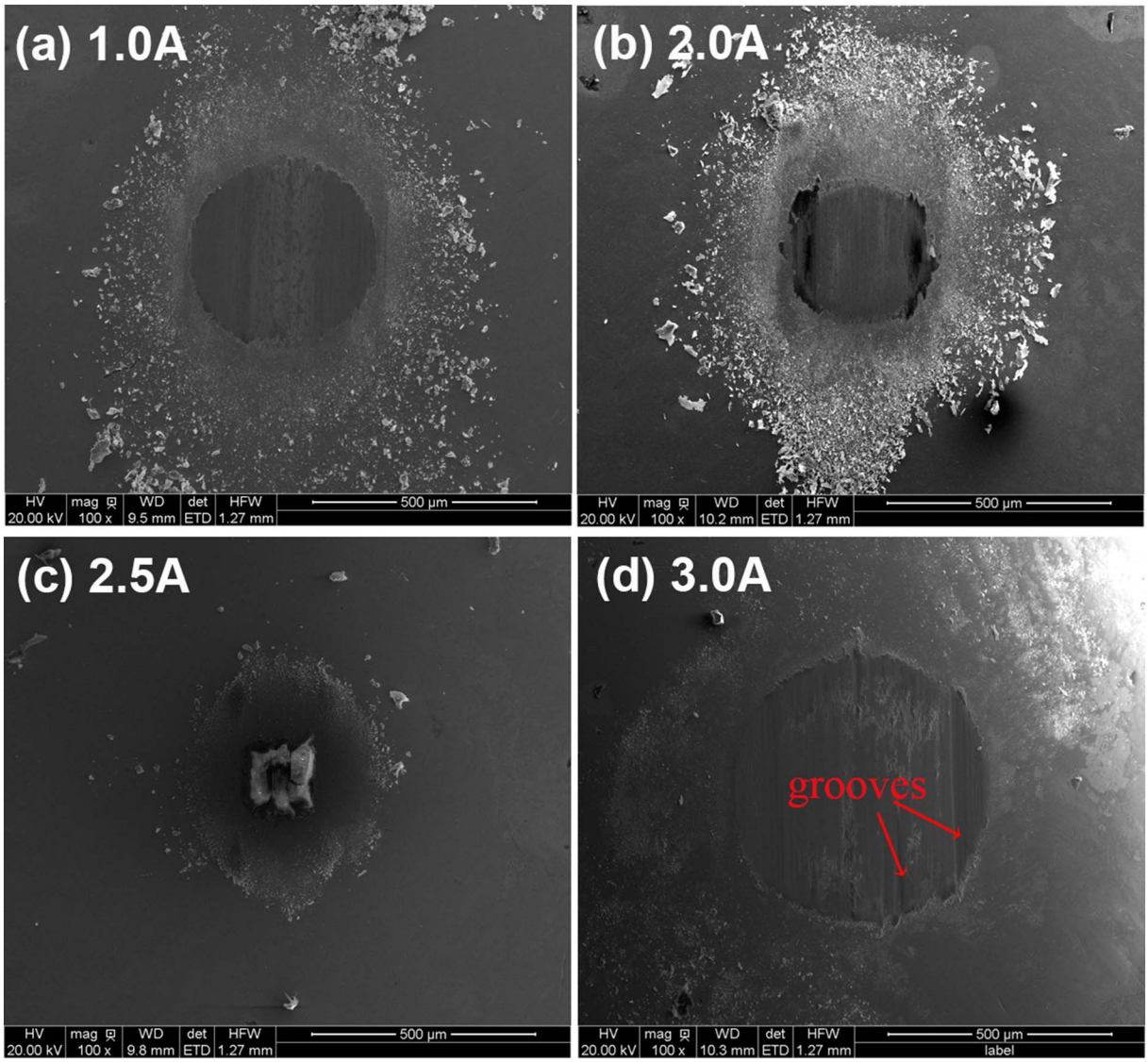

Fig. 7. SEM morphology of wear scars on the steel ball. (For interpretation of the references to color in this figure, the reader is referred to the web version of this article.)

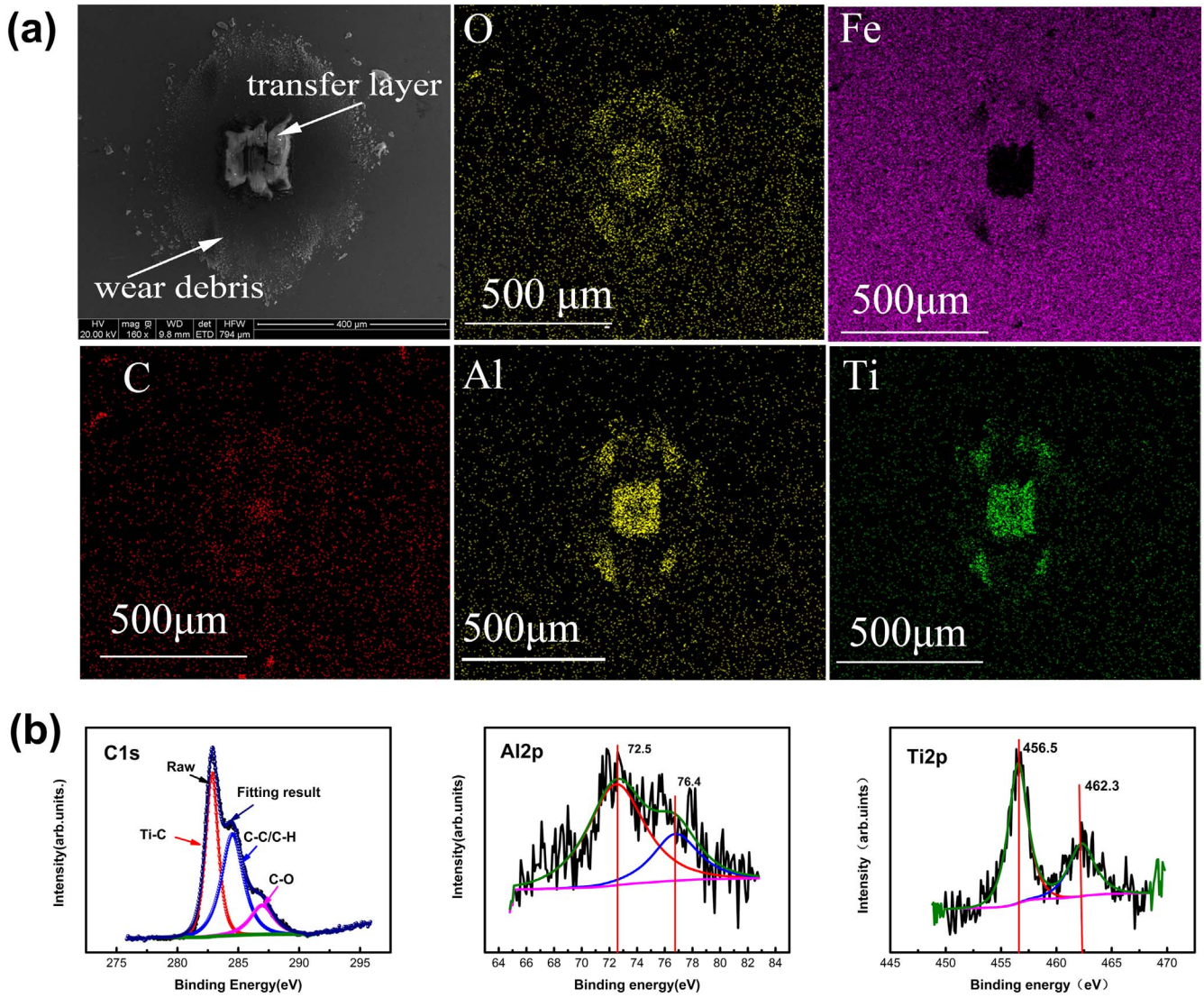

Fig. 8. (a) SEM images and the distribution of C, O, Ti, Al elements of the wear scar on the counterpart and (b) XPS C1s, Al2p and Ti2p spectra of the transfer layer for the case at 2.5 A.

current increased first and then underwent a small dip because sp^2-C was more favorable to bond with the carbide-forming Ti atoms to form titanium carbide than sp^3-C [22]. For the wear tracks, both the I_D/I_G ratio and G peak position as a function of sputtering current increased gradually, suggesting that the sp^2/sp^3 ratio increased and the structure tended to be graphitizing. In particular, the I_D/I_G of wear tracks was much higher than that of the corresponding as-deposited Ti/Al-DLC films, indicating the occurrence of friction-induced graphitization due to the localized rise of temperature at asperity contacts and shear stress during the friction process [23,24], which was normally considered to play a critical role on the superior tribological properties [14,22].

Furtherly, the wear scars on the counterpart were investigated for each case. Fig. 7 shows the wear scars on the mated balls characterized by SEM. For the films at 1.0 and 2.0 A, the wear scars on the counterpart were surrounded by large amount of wear debris. However, a continuous and compact transfer layer was generated on the steel ball sliding against the film at 2.5 A, as will be described later, which provided positive effect on the low friction coefficient. For the case at 3.0 A, the largest wear scar was generated and some wear grooves (identified by the red arrows in Fig. 7d) could be observed clearly, attributing to the formed hard titanium carbide nanoparticles in the as-deposited film (Fig. 3), which was consistent with previous study [20]. In addition, Raman spectra of transfer layers for each case (see Fig. S2 in Supporting Information) confirmed that the peak intensity with sputtering current from 1 to 2.5 A decreased quickly, indicating the significant reduction of C concentration in transfer layer, and there was no transfer layer generated for the case at 3.0 A due to the absence of Raman spectra.

Based on the abovementioned analysis, the structural graphitization of wear tracks occurred for each case (Fig. 6), but the transfer layer was only generated for the film deposited at 1.0, 2.0 and 2.5 A, respectively (Fig. 7). In particular, only Ti/Al-DLC film deposited at 2.5 A exhibited the most excellent tribological properties under air condition (Fig. 4), for which the structure of formed compact transfer layer should be a key issue. So, the further in-depth analysis on the

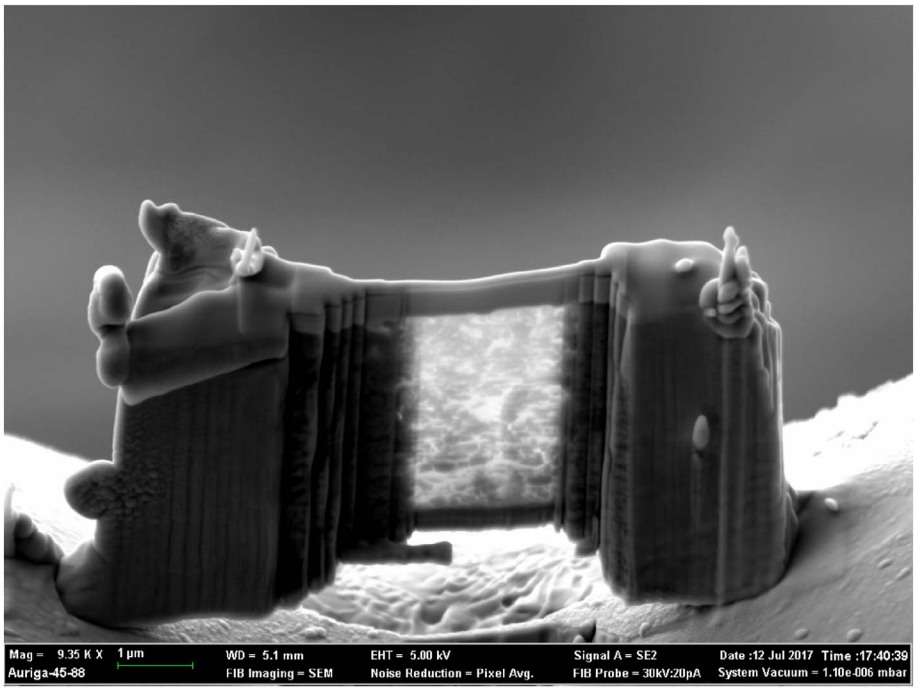

Fig. 9. SEM image of cross section of the transfer layer in the wear scar on the counterpart sliding on the film deposited at 2.5 A.

transfer layer for this case was required to reveal the composition, distribution and existing state of C, Ti and Al, and phase structure, which was indispensable for clarifying the fundamental tribological mechanism.

For the film at 2.5 A, the element distribution and chemical bonds of transfer layer on the counterpart were characterized by EDS and XPS separately, as shown in Fig. 8. The EDS analysis in Fig. 8a confirmed that the transfer layer was composed of C, Ti, Al and O, and the Ti/Al ratio was about 1:1 compared with the as-deposited film (2:1), suggesting that more Ti atoms were consumed in the interface. In Fig. 8b, the C1s spectra was fitted into three components located at the binding energies of 284.6 eV for C-H/C-C, 282.6 eV for Ti—C and 287.9 eV for C═O, respectively [18,19,25,26]. For Al2p spectra, a major peak appeared at about 72.5 eV and a shoulder peak was located at around 76.5 eV after Ar^+ bombardment which corresponded to pure Al and Al—O, respectively [27], suggesting that Al mainly existed in the state of pure and oxidized Al clusters in the transfer layer. For Ti2p spectra, the peaks at 456.5 ± 0.2 eV and 462.3 ± 0.2 eV can be identified as the $Ti2p_{3/2}$ and $Ti2p_{1/2}$ peaks of titanium carbide separately [21]. It has been reported that the binding energies of $Ti2p_{3/2}$ and $Ti2p_{1/2}$ peaks in TiC were around 455.1 and 460.6 eV separately, while the peak positions in TiO_2 were located at around 458.7 eV for $Ti2p_{3/2}$ and 464.5 eV for $Ti2p_{1/2}$, respectively [21,28]. The deviation of obtained Ti2p peak positions to higher binding energies indicated the presence of titanium oxide [21]. Therefore, this XPS result revealed that compared with the as-deposited case, a large amount of Ti atoms bonded with C in the transfer layer following a small amount of titanium oxide, while Al existed as pure and oxidized Al clusters.

Further, the microstructure of transfer layer was characterized by TEM and EDS. Fig. 9 shows the SEM image of cross-section of the formed transfer layer prepared using FIB, which was picked from a relatively uniform part on the steel ball. Based on the sample, the TEM images, corresponding SAED pattern and EDS were obtained, respectively, as given in Fig. 10. From the HRTEM image (Fig. 10a), the transfer layer of about 3 µm was observed, which was much thicker than the as-deposited Ti/Al-DLC film, implying an accumulation process of wear debris in the interface between the DLC and steel ball during the friction process. In the transfer layer, two segregated areas existed, in which the black one was labeled as “A” and the white one was labeled as “B”. By EDS (Table 3) and STEM mapping (Fig. 10b) analysis, the area A mainly contained C, Ti, Al and O, while the area B was mainly composed of C and O, and the carbon concentration in area B reached to 88.00 at.%, which was 4 times higher than that in area A. Besides, HRTEM (Fig. 10a) confirmed that in the area A, many lattice fringes were observed clearly and the sharp crystalline diffraction rings also appeared in the corresponding SAED, which were identified to be TiC(111), TiC(200), Al_2O_3(1211), Al(220) and Ti(311) [19,29] separately. While the area B showed a typical amorphous structure, but some onion-like clusters were observed, which may act as solid lubricant explaining for the low friction coefficient and stable wear [30]. Therefore, compared with the intrinsic Ti/Al-DLC film in which small amount of nanocrystallite embedded in amorphous carbon, the transfer layer had an evident structural transformation and formed a dual nanostructure constructed of cross-linked amorphous carbon networks and predominated crystalline nanoparticulate. Moreover, the interface between the transfer layer and steel ball (labeled as area “C”) was rich in metals, which could improve the adhesion between the transfer layer and steel ball; in the top surface of the transfer layer (labeled as area “D”), it was also covered by the metal-rich layer completely, which contacted with the wear track directly for shearing action.

Based on the systematical evaluation of wear track, wear scar and transfer layer, both of Al and Ti atoms could decide the tribological performance of Ti/Al-DLC films and also affect the formation of transfer layer. In general, Al atoms could promote the segregation of graphitic carbon phase to form a graphitic tribo-layer with low shear strength

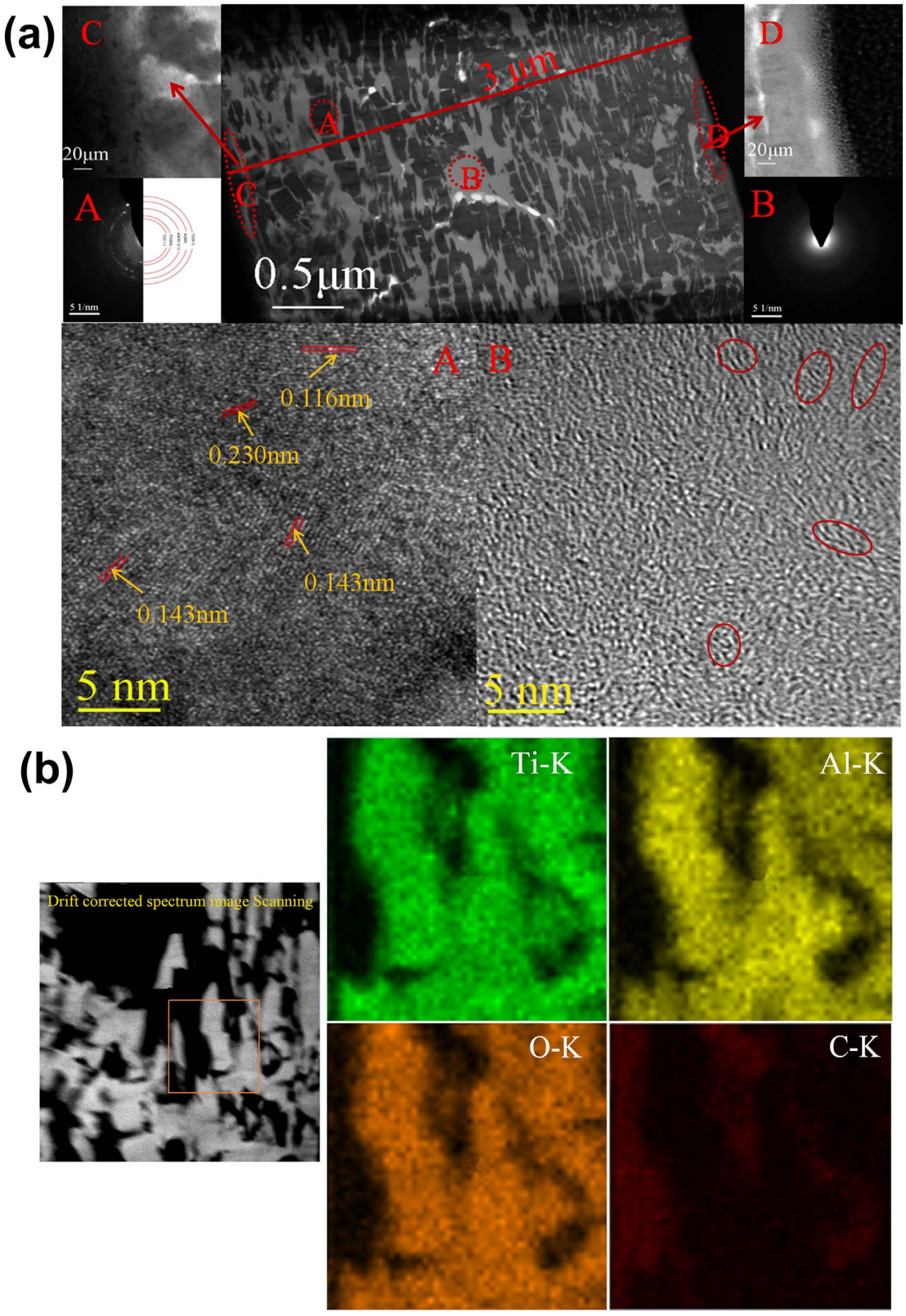

Fig. 10. (a) TEM images of transfer layer and corresponding SAED and (b) STEM mapping for case at 2.5 A in the selected area.

Table 3
Element concentration of the area A and B in the transfer layer.

	Area A/at.%	Area B/at.%
C	21.51	88.00
Ti	10.67	0.34
Al	14.16	0.32
O	53.64	11.33

due to the elevated temperature during sliding friction [10]. For the Ti/Al-DLC films deposited at 1.0 and 2.0 A which had low Al concentration (< 4.4 at.%), the films exhibited higher friction coefficient (Fig. 4) following lower graphitization level during the friction process (Fig. 6) [18,24]. However, for the film deposited at 3.0 A with the maximal Ti/Al concentrations, although the friction-induced graphitization in the wear track was the most remarkable than other cases, the worse tribological property shown in Fig. 4 was achieved, attributing to two factors where one was the absent of transfer layer (Fig. S2 in Supporting Information) on the counterpart due to the low C concentration in the as-deposited film and the other was the formed large amount of hard titanium carbide nanoparticles [19].

However, the film deposited at 2.5 A exhibited the best tribological properties (Fig. 4), and its tribological mechanism could be explained as following. As shown in Fig. 11, during the friction process, the obvious graphitization occurred in the wear track region due to the proper Al concentration (Fig. 6), and then a continuous and dense transfer layer was formed and adhered to the counterpart (Fig. 10). Especially, the doped Al in the transfer layer mainly existed in the state of pure and oxidized Al clusters (Fig. 8), while the pure metal Al could be dissolved into TiC matrix at elevated temperatures [31–33] and created a driving force for the separation of carbide particle from the amorphous carbon matrix, which resulted in a dual nanostructure of cross-linked amorphous carbon networks and predominated crystalline nanoparticulate (Fig. 10). This special structure afforded more interfaces to promote the sheared slippage occurred easily, contributing to the best friction properties. Besides, highly reactive Al tended to be interacted with oxygen/H_2O in the air during the sliding process, causing the high concentration of aluminum oxide in the transfer layer (Fig. 10). As reported [34,35], metal carbide or oxide layers enriched on the film surface could prevent the incursion and destruction of O to the cross-linked carbon network, and thus the oxidation resistance of DLC films could be greatly enhanced, which explained the lowest wear rate of deposited film.

4. Conclusions

Ti/Al-DLC films with different co-doped concentrations were successfully fabricated on silicon substrates using hybrid ion beam system, and the composition, microstructure and tribological properties of films were analyzed systematically. Results revealed that the elemental compositions of Ti/Al-DLC films were tailored by sputtering current. In the as-deposited films, the doped Al mainly existed as the pure and oxidized clusters in the amorphous carbon structures for each case, while the Ti gave the different evolution of chemical state. When the sputtering current was 1.0 and 2.0 A, the Ti dissolved in the amorphous carbon without crystalline structure generated, and the films exhibited higher friction coefficient following lower graphitization level due to the low Al concentration (< 4.4 at.%). With the sputtering current increased to 2.5 and 3.0 A, the hard titanium carbide was formed in the films; although for the film at 3.0 A the friction-induced graphitization on the wear tracks was enhanced, the absent of transfer layer on the counterpart and the large amount of hard titanium carbide nanoparticles deteriorated the tribological properties seriously. However, the Ti/Al-DLC film deposited at 2.5 A ($Ti_{10.06\%}Al_{4.78\%}$) exhibited the lowest friction coefficient of 0.05 and wear rate of $1.56 \times 10^{-16}\ m^3\ N^{-1}\ m^{-1}$, which originated from the formation of continuous thicker transfer layer with a dual nanostructure of cross-linked amorphous carbon networks and predominated crystalline nanoparticulate (mainly TiC and Al_2O_3) in the interface.

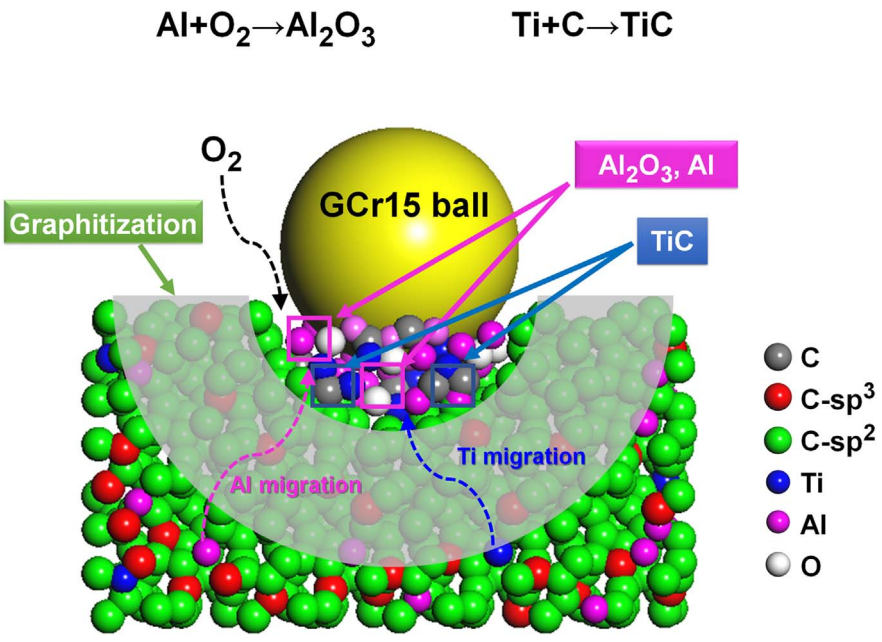

Fig. 11. A schematic representation of tribological mechanism of Ti/Al-DLC film against steel ball under atmospheric environment condition.

Acknowledgements

This research was supported by the National Natural Science Foundation of China (51522106, 51772307), National Key R&D Program of China (2017YFB0702303), and the Korea Research Fellowship Program funded by the Ministry of Science and ICT through the National Research Foundation of Korea (2017H1D3A1A01055070).

Appendix A. Supplementary data

Raman spectra of the as-deposited Ti/Al-DLC and wear tracks as a function of sputtering current (Fig. S1); Raman spectra of the transfer layers on the steel ball (Fig. S2). Supplementary data associated with this article can be found in the online version, at https://doi.org/10.1016/j.surfcoat.2018.02.098.

References

[1] J. Robertson, Diamond-like amorphous carbon, Mater. Sci. Eng. 37 (2002) 129–281.
[2] J. Wang, J. Pu, G. Zhang, L. Wang, Interface architecture for super thick carbon based films toward low internal stress and ultrahigh load-bearing capacity, ACS Appl. Mater. Interfaces 5 (11) (2013) 5015–5024.
[3] W.J. Yang, T. Sekino, K.B. Shim, Deposition and microstructure of Ti-containing diamond-like carbon nanocomposite films, Thin Solid Films 473 (2) (2005) 252–258.
[4] A.Y. Wang, K.R. Lee, J.P. Ahn, Structure and mechanical properties of W incorporated diamond-like carbon films prepared by a hybrid ion beam deposition technique, Carbon 44 (9) (2006) 1826–1832.
[5] M.C. Chiu, W.P. Hsieh, W.Y. Ho, Thermal stability of Cr-doped diamond-like carbon films synthesized by cathodic arc evaporation, Thin Solid Films 476 (2) (2005) 258–263.
[6] G.A. Zhang, P.X. Yan, P. Wang, The effect of applied substrate negative bias voltage on the structure and properties of Al-containing a-C:H thin films, Surf. Coat. Technol. 202 (12) (2008) 2684–2689.
[7] S. Dub, Y. Pauleau, F. Thièry, Mechanical properties of nanostructured copper-hydrogenated amorphous carbon composite films studied by nanoindentation, Surf. Coat. Technol. 180–181 (2004) 551–555.
[8] H. Zhou, Q.Y. Hou, T.Q. Xiao, Y.D. Wang, The composition, microstructure and mechanical properties of Ni/DLC nanocomposite films by filtered cathodic vacuum arc deposition, Diam. Relat. Mater. 75 (2017) 96–104.
[9] J. Huang, L. Wang, B. Liu, S. Wan, Q. Xue, In vitro evaluation of the tribological response of Mo-doped graphite-like carbon film in different biological media, ACS Appl. Mater. Interfaces 7 (4) (2015) 2772–2783.
[10] S.G. Zhou, L.P. Wang, Z.B. Lu, Q. Ding, S.C. Wang, Robert J.K. Wood, Q.J. Xue, Tailoring microstructure and phase segregation for low friction carbon-based nanocomposite coatings, J. Mater. Chem. 22 (2012) 15782.
[11] M. Paranjayee, P.E. Arutiun, E.H. Papken, Tribological behaviour of Mo–W doped carbon-based coating at ambient condition, Tribol. Int. 90 (2015) 135–147.
[12] X.Q. Liu, J.Y. Hao, J. Yang, J.Y. Zheng, Y.M. Liang, W.M. Liu, Preparation of superior lubricious amorphous carbon films co-doped by silicon and aluminum, J. Appl. Phys. 110 (2011) 053507.
[13] X.W. Li, L.L. Sun, P. Guo, P.L. Ke, A.Y. Wang, Structure and residual stress evolution of Ti/Al, Cr/Al or W/Al co-doped amorphous carbon nanocomposite films: insights from ab initio calculations, Mater. Des. 89 (2016) 1123–1129.
[14] C.L. Chang, J.Y. Jao, T.C. Chang, Influences of bias voltage on properties of TiAl-doped DLC coatings synthesized by cathodic arc evaporation, Diam. Relat. Mater. 14 (11–12) (2005) 2127–2132.
[15] T. Guo, C.C. Kong, X.W. Li, P. Guo, A.Y. Wang, Microstructure and mechanical properties of Ti/Al co-doped DLC films: dependence on sputtering current, source gas, and substrate bias, Appl. Surf. Sci. 410 (2017) 51–59.
[16] X.W. Li, P. Guo, L.L. Sun, X. Zuo, D. Zhang, P.L. Ke, A.Y. Wang, Ti/Al co-doping induced residual stress reduction and bond structure evolution of amorphous carbon films: an experimental and ab initio study, Carbon 111 (2017) 467–475.
[17] X. Pang, L. Shi, P. Wang, Effects of Al incorporation on the mechanical and tribological properties of Ti-doped a-C:H films deposited by magnetron sputtering, Curr. Appl. Phys. 11 (2011) 771–775.
[18] V. Singh, J.C. Jiang, E.I. Meletis, Cr-diamond like carbon nanocomposite films: synthesis, characterization and properties, Thin Solid Films 489 (1–2) (2005) 150–158.
[19] W. Dai, P.L. Ke, M. Moon, Investigation of the microstructure, mechanical properties and tribological behaviors of Ti-containing diamond-like carbon films fabricated by a hybrid ion beam method, Thin Solid Films 520 (19) (2012) 6057–6063.
[20] J.Y. Won, S. Tohru, B.S. Kwang, Deposition and microstructure of Ti-containing diamond-like carbon nanocomposite films, Thin Solid Films 473 (2) (2005) 252–258.
[21] R.A. Alawajji, G.K. Kannarpady, Z.A. Nima, N. Kelly, F. Watanabe, A.S. Biris, Electrical properties of multilayer (DLC-TiC) films produced by pulsed laser deposition, Appl. Surf. Sci. (2017), http://dx.doi.org/10.1016/j.apsusc.2017.08.058.
[22] X. Pang, L. Shi, P. Wang, Y. Xia, W. Liu, Influence of methane flow on the microstructure and properties of TiAl-doped a-C: H films deposited by middle frequency reactive magnetron sputtering, Surf. Interface Anal. 41 (2009) 924–930.
[23] F. Zhao, H. Li, L. Ji, Y. Wang, Ti-DLC films with superior friction performance, Diam. Relat. Mater. 19 (2010) 342–349.
[24] Y. Liu, A. Erdemir, E.I. Meletis, An investigation of the relationship between graphitization and frictional behavior of DLC coatings, Surf. Coat. Technol. 86–87 (1996) 564–568.
[25] W. Dai, P.L. Ke, A.Y. Wang, Microstructure and property evolution of Cr-DLC films with different Cr content deposited by a hybrid beam technique, Vacuum 25 (2011) 792–797.
[26] K. Baba, R. Hatada, Deposition and characterization of Ti- and W-containing diamond-like carbon films by plasma source ion implantation, Surf. Coat. Technol. 169 (2003) 287–290.
[27] NIST XPS data base, Selected Element Search Result, https://srdata.nist.gov/xps/ElmComposition.aspx, (2018) , Accessed date: 18 January 2010.
[28] Q.Z. Wang, F. Zhou, Z.F. Zhou, Y. Yang, C. Yan, C.D. Wang, Influence of Ti content on the structure and tribological properties of Ti-DLC coatings in water lubrication, Diam. Relat. Mater. 25 (2012) 163–175.
[29] F.S. Alencastro, E.S. Jr, M.E. Mendoza, J.R. Araújo, S. Suarez, B.S. Archanjo, R.A. Simão, Hardening of Al thin films by Ti-C doping, Surf. Coat. Technol. 325 (2017) 650–655.
[30] I.C. Müller, J. Sharp, W.M. Rainforth, P. Hovsepian, A. Ehiasarian, Tribological response and characterization of Mo–W doped DLC coating, Wear 376–377 (2017) 1622–1629.
[31] O. Wilhelmsson, M. Råsander, M. Carlsson, E. Lewin, B. Sanyal, U. Wiklund, O. Eriksson, U. Jansson, Design of nanocomposite low-friction coatings, Adv. Funct. Mater. 17 (2007) 1611–1616.
[32] M. Lindquist, O. Wilhelmsson, U. Jansson, U. Wiklund, Tribofilm formation and tribological properties of TiC and nanocomposite TiAlC coatings, Wear 266 (2009) 379–387.
[33] M. Lindquist, O. Wilhelmsson, U. Jansson, U. Wiklund, Tribofilm formation from TiC and nanocomposite TiAlC coatings, studied with focused ion beam and transmission electron microscopy, Wear 266 (2009) 988–994.
[34] I.L. Singer, I.L. Singer, H.M. Pollock (Eds.), Fundamentals of Friction: Macroscopic and Microscopic Process, Kluwer Academic Publishers, Netherlands, 1992, p. 237.
[35] L. Ji, H. Li, F. Zhao, W. Quan, J. Chen, Atomic oxygen resistant behaviors of Mo/diamond-like carbon nanocomposite lubricating films, Appl. Surf. Sci. 255 (2009) 4180.